05

Nanodomain engineering in LNOI thin films on the nonpolar surface

© Ya.V. Bodnarchuk, R.V. Gainutdinov, T.R. Volk

Shubnikov Institute of Crystallography of Kurchatov complex „Crystallography and photonics"of NRC „Kurchatov institute", 119333 Moscow, Russia
e-mail: deuten@mail.ru

Received September 5, 2024
Revised October 15, 2024
Accepted October 17, 2024

Micro- and nanodomain structures were written by AFM-tip voltages on the nonpolar (X) surface using special in LNOI thin film ($LiNbO_3$-on-insulator). Properties of structures recording have been investigated and discussed. The domain structures investigation was carried out by the PFM method. The dependences of the domain length on the pulse duration and voltage are obtained, them well approximated by exponential and linear functions, respectively. Piezoelectric hysteresis loops were measured and coercive and bias voltages were estimated. Analysis of hysteresis loops showed that the values of coercive and bias voltages are practically independent on the time of the voltage pulse applied to the AFM tip

Keywords: domain structures, thin film, atomic force microscopy, lithium niobate.

DOI: 10.61011/TP.2025.01.60509.270-24

Introduction

An urgent task today is the search for ferroelectric materials and their derivatives as working nonlinear photonic crystals. Currently, two main directions in this field of research can be distinguished, such as domain-wall conductivity (DWC) and nonlinear transformation of optical radiation on a domain structure in the quasi-phase matching mode (QPM). Currently, there are at least two most suitable objects for solving these tasks. These are Ne:$LiNbO_3$, Ti:$LiNbO_3$ and helium implanted optical waveguides formed on nonpolar (X- and Y-) surfaces of crystal $LiNbO_3$ [1–5], as well as thin single-crystal films of $LiNbO_3$ ($LiNbO_3$-on-insulator) LNOI [6–9] transferred to a layered structure — lithium niobate single crystal with a thin layer of SiO_2, and in some cases with a metal layer. The waveguide effect in a thin film is achieved due to the difference in refractive indices SiO_2 and $LiNbO_3$. The regular operating domain structure is formed either by exposure to the electron beam of a scanning electron microscope, or by applying voltage to the tip of the probe of an atomic force microscope (AFM). The kinetics of recording individual domains depending on the modes of exposure to an electron beam (accelerating voltage, exposure time, beam current) has been studied quite well both on lithium niobate single crystals and on optical waveguides based on it, and on polar and nonpolar surfaces. The domain originated at the irradiation point grows along the Z axis in case of electron irradiation of a nonpolar surface. The driving force is the tangential component E_z of the space charge field E_{sc} induced by an electron beam at the irradiation point; the layer thickness is determined by the accelerating voltage U [1,10].

There is also a sufficient number of papers about the kinetics of domain switching under the impact of the AFM-tip voltages on the polar surfaces of LNOI films of various thicknesses. For instance, dependences of the domain size on the magnitude and duration of the exposure of the voltage pulse applied to the AFM tip were obtained in Ref. [6–8]. Local piezoelectric hysteresis loops were also measured at different pulse durations of the applied voltage. Detailed methods for measuring local hysteresis loops can be found in a variety of papers [11,12]. The effect of ambient humidity on the kinetics of the formation of single domains and regular domain structures is discussed in Ref. [13]. Nevertheless, it is preferable to use nonpolar thin film surfaces to implement nonlinear optical radiation transformation on a domain structure in the QPM mode. There are also few papers covering the formation of a regular domain structure (RDS) on nonpolar surfaces of LNOI [14–16], but RDS in these studies was recorded by applying a field to external electrodes, followed by their study by piezoelectric force microscopy and conducting AFM. According to our concepts, the kinetics of the formation of single domains in the AFM-tip voltages has not been studied before. Thus, the task in this paper was to study the kinetics of the formation of single domains in the AFM-tip voltages on the nonpolar surface of LNOI films for obtaining a more complete picture of the microscopic mechanisms of domain formation.

1. Samples and experimental techniques

Thin LNOI ($LiNbO_3$-on-insulator) films of nonpolar (X-) orientation were used in this experiment. The thickness of the waveguide layer of $LiNbO_3$ is 703.5 nm in the studied samples, the thickness SiO_2 is 1.905 μm; the total size of the samples is $X \times Y \times Z = 0.5 \times 10 \times 10$ mm.

The domains were recorded in the AFM-tip voltages followed by examination by piezoelectric force microscopy (PFM) using NTEGRA Prima microscope (NT-MDT Spectrum Instruments, Zelenograd) in a clean area of the control

and measuring complex „TRACKPORE ROOM-05“ (purity class 5 ISO (100), accuracy of maintaining the temperature (T) in the ambient air in the clean zone in the range of 25 ± 5°C was ± 0.05°C, the relative humidity in the range of $40 \pm 10\%$ was maintained with an accuracy of $\pm 1\%$). The experiments used silicon cantilevers (HA_FM, beam B, LLC„Kapella“, Zelenograd) coated with Pt, which had the following characteristics: resonant frequency $f = 77$ kHz, stiffness $k = 3.5$ N/m, point rounding radius $R < 35$ nm. The domain structure was studied in the lateral PFM mode. The domains were recorded using the application of a constant voltage U_{DC} AFM tip in an LNOI thin film and are schematically shown in Fig. 1. The domains were recorded by using the vector lithography method according to a graphic template created in advance with different recording intervals by applying U_{DC} between a conductive tip in contact with a nonpolar (X-) surface. Local piezoelectric hysteresis loops $H_\omega - U_{DC}$ were obtained by applying voltage pulses U_{DC} with varying amplitude from $+50$ to -50 V and then from -50 to $+50$ V with an amplitude step of 100 mV (H_ω — electromechanical response signal). The duration of the voltage pulses t_p, constant for this cycle, ranged from 10 to 1000 ms for different cycles, the pulse interval 10 ms. The piezoelectric response signal was measured in the interval between pulses at $U_{DC} = 0$ V.

2. Results and discussions

2.1. Writing domains in an LNOI thin film using AFM

Lithium niobate $LiNbO_3$ has not been studied well enough on a microscopic scale due to significantly high coercive fields $E_c = 220$ kV/cm in congruent and 60 kV/cm in stoichiometric composition. Therefore, such materials as thin films of LNOI ($LiNbO_3$-on-insulator) provide a great advantage in understanding the processes in the basic optoelectronics material. The LNOI thin film is promising for a number of applications [17–20], and is also suitable for studying switching processes, hysteresis loops, and related ferroelectric effects. The use of modern AFM methods for the diagnostics and study of LNOI thin films provides a number of advantages in understanding the processes in more detail. Fig. 1 shows a block diagram of a structure containing an LNOI thin film, a layer of silicon oxide SiO_2, and a subsequent three-dimensional $LiNbO_3$ crystal. Fig. 1 illustrates the recording of domains on an LNOI thin film of nonpolar (X-) orientation with an AFM tip.

Next, we will discuss in more detail the processes of AFM recording on a nonpolar slice in an LNOI thin film. The domains recorded with the AFM tip are stable and do not degrade during the observation period (several months). Fig. 2 shows PFM images of recorded single domains using AFM vector lithography. The domain that originated at the recording point grows frontally along the polar axis $+Z$ in a thin layer under the action of the tangential component of

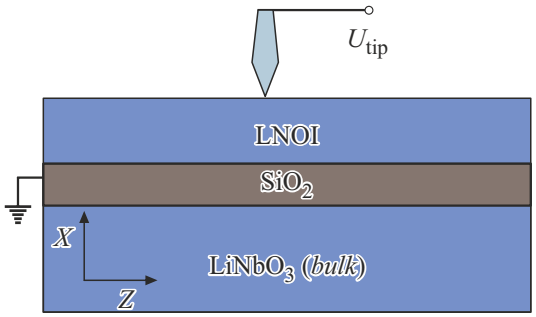

Figure 1. Diagram of recording domains with an AFM tip in an LNOI thin film of nonpolar (X-) orientation.

the field E_z created at the point of contact of the AFM tip with the surface. The domain is elongated along the polar axis Z in Fig. 2, the domain itself is shaped like a „drop or needle“, where $L \gg D$, and the domain is wider at the recording point than at the other edge (L — length of the domain along the polar axis, D — width in the orthogonal direction). The process of domain formation during local recording with an AFM tip is similar to the process of domain formation during electron irradiation, where the needle-like shape of the domain during electron beam recording has been demonstrated in many papers [2,10].

The domains were visualized in PFM mode after the domain recording, and the recorded single domain structures were calculated at different pulse durations $t_p = 500-5000$ ms. The domain sizes were calculated in the SPIP program after recording. The dependences of the domain length on the pulse duration are shown in Fig. 3.

The domains were recorded in the voltage range of $U_{DC} = 30-50$ V, where domains with the voltage of less than 30 V were not visualized. The data was approximated by the exponential function $y = k \exp(x/t) + y_0$. Fig. 3 shows the difference in the growth curves for domains recorded at 30 V, and for domains recorded at 40–50 V. The saturation yield of the curve for data at 30 V is characterized by a lower coefficient $k = 26$ and time $t = 929$ s, which may be the cause of nucleation and subsequent frontal growth only in a thin near-surface layer. Whereas coefficient $k = 282$ and time $t = 471$ s for 40 V, coefficient $k = 249$ and time $t = 349$ s for 50 V. It can be seen from these coefficients that switching occurs at shorter times t_p at a higher voltage and the switching process for 40–50 V is almost the same. This domain growth takes place in low and medium fields, according to the exponential function.

Next, the dependences of the domain length $L_D(U_{DC})$ for $t_p = \text{const}$ shown in Fig. 4 were studied.

These dependences $L(U_{DC})$ are well described by a linear function, which was obtained earlier in the study of thin films of polar orientation [7,8]. The domains appear at certain threshold voltages U_{thr} (in our case ≥ 30 V), which decreases with the increase of the pulse duration. However, a certain pulse duration is required to consolidate the formed domains, whereas they disappear with shorter t_p.

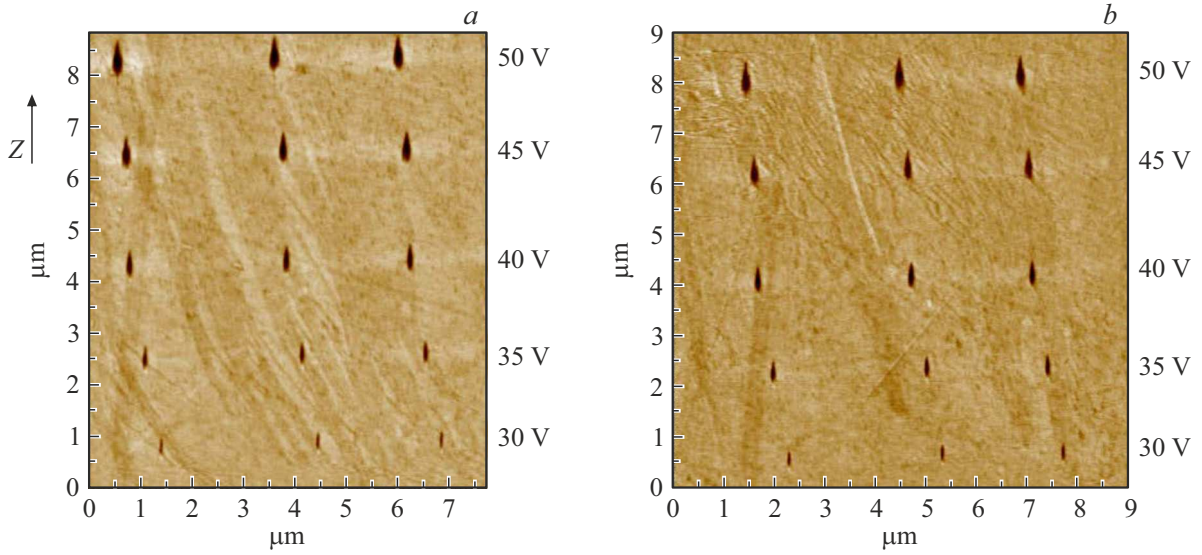

Figure 2. PFM images of recorded single domains using AFM vector lithography: *a* — pulse duration $t_p = 1$ s; *b* — pulse duration $t_p = 5$ s; voltage $U_{DC} = 30-50$ V.

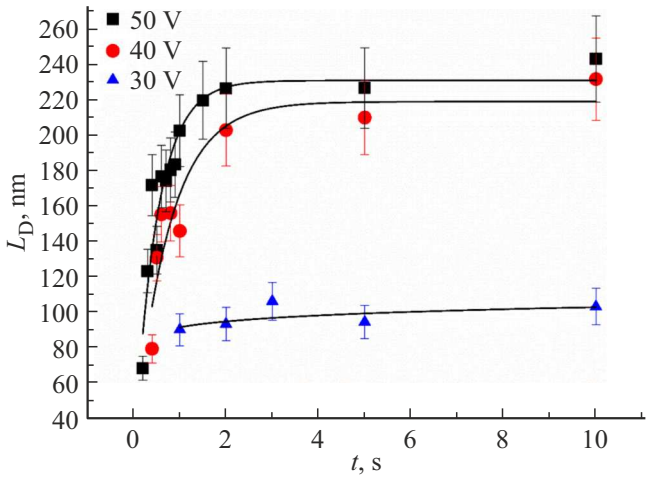

Figure 3. Dependence of domain length L_D on the pulse duration at voltages $U_{DC} = 30-50$ V.

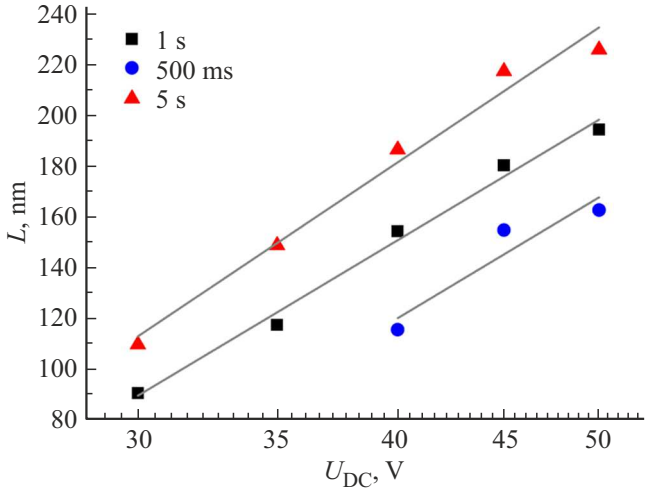

Figure 4. Dependence of the domain length on voltage $L(U_{DC})$ at $t_p = 500$ ms, 1 and 5 s, respectively.

This shows the reverse switching effect characteristic of $LiNbO_3$ [21].

2.2. Hysteresis loops

Let us consider a question related to hysteresis loops. Piezoelectric hysteresis loops were obtained using indirect measurement (AFM methods), where the observed shape of the hysteresis loop cannot be directly interpreted in terms of spontaneous polarization P_s and coercive field E_c. However, the amplitude and width of the loops qualitatively characterize the residual polarization P_{rem} and the coercive voltage U_c. Fig. 5 shows the results of studies of LNOI hysteresis loops in the range of pulse duration t_p from 10 to 1000 ms. The loops obtained under the given conditions were measured at closely spaced surface points within a single AFM scan. The loops observed in LNOI are strongly shifted and unipolar, however, P_{rem} does not increase with an increase of t_p, which indicates that there is no pinning at the domain boundaries or it is very weak. Whereas the distribution of hysteresis loops depends on the loop frequency in the helium implanted waveguide He:$LiNbO_3$ [22], and the hysteresis loops are spatially scattered, as evidenced by the apparent pinning on the waveguide (locking) layer.

The coercive voltage U_c and the bias voltage U_b listed in the table were calculated based on the obtained hysteresis loops. It can be seen from these data that U_c slightly decreases with an increase of t_p, which may be an instrument measurement error ($< 10\%$), and not associated

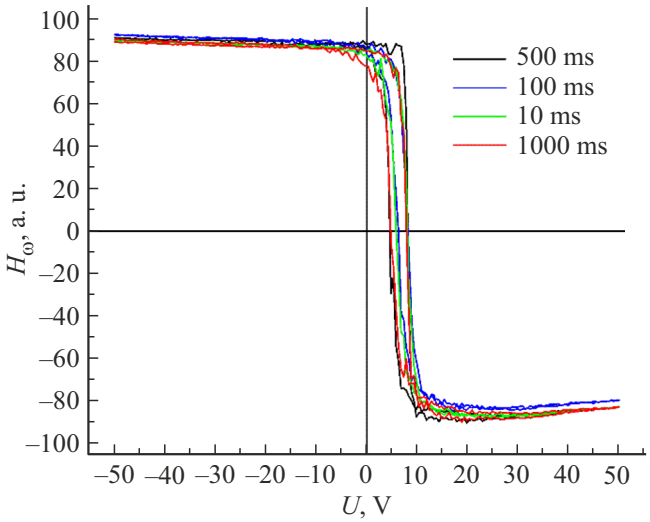

Figure 5. Piezoelectric hysteresis loops in LNOI, obtained at closely spaced surface points at t_p from 10 to 1000 ms.

U_b and U_c, obtained from hysteresis loops

t_p, ms	U_c, V	U_b, V
10	7.32	1.093
100	7.046	0.987
500	6.168	1.582
1000	6.49	1.45

with pinning on the interface. No reverse switching and an increase of the bias voltage U_b compared with a bulk crystal was observed in previously published papers on switching thin LNOI films with a layer of gold [6].

Conclusion

Microdomain structures were recorded in an LNOI thin film ($LiNbO_3$-on-insulator) of nonpolar (X-) orientation with a thickness of 703.5 nm using an AFM tip and their properties were investigated. The obtained dependences of the domain length L_D on the pulse duration t_p and voltage U_{DC} were approximated by exponential and linear functions, respectively, which shows the similarity in kinetics in the previously obtained results on thin films (Z-) and in a helium-implanted waveguide (Z-) orientation. It has been shown that domains appear at a threshold voltage of 30 V and above, since either reverse switching occurs at the voltage up to < 30 V, or domain pinning does not occur on the interface. The switching takes place at shorter pulse durations t_p when the voltage increases. It was found that the coercive voltage and the displacement field are practically independent of the pulse application time, which indicates similar mechanisms in polar and nonpolar sections. The stability of the recorded domain structures are in good agreement with the previously obtained results in lithium niobate and its derivative structures.

Funding

The study was performed under the State assignment of National Research Center „Kurchatov Institute“.

Acknowledgments

The study was performed under the state assignment of National Research Center „Kurchatov Institute“ using the equipment of CUR „Structural Diagnostics of Materials“.

Conflict of interest

The authors declare that they have no conflict of interest.

References

[1] L.S. Kokhanchik, M.V. Borodin, S.M. Shandarov, N.I. Burimov, V.V. Shcherbina, T.R. Volk. Physics Solid State, **52** (8), 1722 (2010). DOI: 10.1134/S106378341008024X
[2] L.S. Kokhanchik, M.V. Borodin, N.I. Burimov, S.M. Shandarov, V.V. Shcherbina, T.R. Volk. IEEE Transactions on Ultrasonics, Ferroelectrics and Waveguide Applications **59**, 1076 (2012). DOI: 10.1109/TUFFC.2012.2298
[3] T.R. Volk, L.S. Kokhanchik, R.V. Gainutdinov, Y.V. Bodnarchuk, S.M. Shandarov, M.V. Borodin. J. Lightwave Tech., **33** (23), 4761 (2015). DOI: 10.1109/JLT.2015.2480496
[4] D. Lavrov, L.S. Kokhanchik, R.V. Gainutdinov, A.S. Elshin, Ya.V. Bodnarchuk, E.D. Mishina, T.R. Volk. Opt. Mater., **75**, 325 (2018). DOI: 10.1016/j.optmat.2017.10.046
[5] S.M. Shandarov, L.S. Kokhanchik, T.R. Volk, E.N. Savchenkov, M.V. Borodin. Quant. Electron., **48**, 761 (2018). DOI: 10.1070/QEL16710
[6] R.V. Gainutdinov, T.R. Volk, H. Zhang. Appl. Phys. Lett., **107**, 162903 (2015). DOI: 10.1063/1.4934186
[7] T.R. Volk, R.V. Gainutdinov, H. Zhang. Appl. Phys. Lett., **110**, 132905 (2017). DOI: 10.1063/1.4978857
[8] T.R. Volk, R.V. Gainutdinov, H. Zhang. Crystals, **7**, 137 (2017). DOI: 10.3390/cryst7050137
[9] R. Gainutdinov, T. Volk. Crystals, **10**, 1160 (2020). DOI: 10.3390/cryst10121160
[10] T.R. Volk, L.S. Kokhanchik, R.V. Gainutdinov, Y.V. Bodnarchuk, S.D. Lavrov. J. Adv. Dielectrics, **8** (2), 1830001 (2018). DOI: 10.1142/S2010135X18300013
[11] A.V. Ankudinov, A.N. Titkov. FTT, **47**, 1110 (2005) (in Russian)
[12] A. Kholkin, S. Kalinin, A. Roelofs, A. Gruverman. *Review of Ferroelectric domain imaging by piezoresponse force microscopy* (Scanning Probe Microscopy. S. Kalinin, A. Gruverman. Ed.: Springer, NY., 2007), p. 173–214.
[13] B.N. Slautin, A.P. Turygin, E.D. Greshnyakov, A.R. Akhmatkhanov, H. Zhu, V.Ya. Shur. Appl. Phys. Lett., **116**, 152904 (2020). DOI: 10.1063/5.0005969
[14] A. Prencipe, K. Gallo. IEEE J. Quant. Electron., **59** (3), 0600108 (2023). DOI: 10.1109/JQE.2023.3234986
[15] D. Sun, Y. Zhang, D. Wang, W. Song, X. Liu, J. Pang, D. Geng, Y. Sang, H. Liu. Light: Sci. Applicat., **9**, 197 (2020). DOI: 10.1038/s41377-020-00434-0

[16] J. Ma, N. Zheng, P. Chen, X. Xu, Y. Zhu, Yu. Nie, Sh. Zhu, M. Xiao, Y. Zhang. Opt. Express, **32** (8), 14801 (2024). DOI: 10.1364/OE.518885
[17] J. Seidel, L.W. Martin, Q. He, Q. Zhan, Y.-H. Chu, A. Rother, M.E. Hawkridge, P. Maksymovych, P. Yu, M. Gajek, N. Balke, S.V. Kalinin, S. Gemming, F. Wang, G. Catalan, J.F. Scott, N.A. Spaldin, J. Orenstein, R. Ramesh. Nat. Mater., **8**, 229 (2009). DOI: 10.1038/nmat2373
[18] G. Catalan, J. Seidel, R. Ramesh, J.F. Scott. Rev. Mod. Phys., **84**, 119 (2012). DOI: 10.1103/RevModPhys.84.119
[19] P.S. Bednyakov, B.I. Sturman, T. Sluka, A.K. Tagantsev, P.V. Yudin. Comp. Mater., **4**, 65 (2018). DOI: 10.1038/s41524-018-0121-8
[20] M. Rusing, P.O. Weigel, J. Zhao, S. Mookhrjea. IEEE Nanotechnol. Magazine, **13**, 18 (2019). DOI: 10.1109/MNANO.2019.2916115
[21] V. Gopalan, Q. Jia, T.E. Mitchell. Appl. Phys. Lett., **75** (16), (1999). DOI: 10.1063/1.125055
[22] Ya.V. Bodnarchuk, R.V. Gainutdinov, T.R. Volk, F. Chen. J. Lightwave Technol., **40**, 5231 (2022). DOI: 10.1109/JLT.2022.3175021

Translated by A.Akhtayamov